

Chapter 5

Skewed Number Plate Recognition using Radon Transform

5.1 Introduction

In the previous chapter, considering the limitations of the existing approaches, a noble approach is proposed for localization, extraction and recognition of the license plate for Vehicular Number Plate Recognition. The proposed methodology is capable to balance these limitations. As per the recent facts, there are several methods to localize license plate, hence post-processing methods are applied to merge all detected regions. Over the last 20 years, the development of Intelligent Transportation System has grown rapidly. The existing approaches for automatic number plate recognition have gained the desired maturity level with respect to the accuracy of recognition.

There are many countries, where the transport rules are either not strictly followed or are made loosely. In such countries, there are possibilities of having variations in number plates with improper locations may be that the license number plate is broken, tilted or both. Some license plate may have dull or unreadable text. To recognize the tilted license plate is a hard job for automatic vehicular number plate recognition. The existing approaches for VNPR assume that the

* The entire chapter in the form of paper has been communicated in “IEEE Computer”, 2014.

text lies in a plane whose angles are normal to the optical axis of the sensor and hence did not consider the tilted situation. In order to extend the application of VNPR into various fields, it is necessary to consider the tilted plate recognition as well. The contribution of this chapter is to propose a method to detect the orientation of the license plate and to rotate the license plate to make it horizontal. Thereafter, the existing methodologies can be used for its recognition.

5.2 Related Work

Jain and Yu [175] extracted the text through color reduction techniques and then applied trained classifier for elimination of non-text components. However the recognition of skewed text was not discussed. Recently Epshtein *et al.* [176] transformed the image content containing color values per pixel to image containing the most likely stroke width through Stroke Width Transform. The accuracy of this algorithm is appreciable for horizontal text detection but the algorithm failed to detect rotated text.

Another approach for recognition of multi-oriented texts in images and video frames has been proposed by Yi and Tian [177]. This approach has two steps. In the first step, the candidate components using gradient and color, the based partition is extracted. In the second step, the line grouping strategy is followed, which aggregates the components into text strings. However, this approach relies on a large set of manually defined rules and thresholds. Further it is assumed that a text string has at least three characters.

Shivakumara *et al.* [178] also proposed an algorithm for oriented text recognition using K-means clustering in the Fourier Laplacian domain. Skeletonization is used to divide the clusters into components. However this approach is limited to detect only text blocks, because of grouping mechanism.

Maximally stable external regions (MSER) based method is proposed by Neumann and Matas [179] for oriented text recognition. However, MSER has failed to include sensitivity to blur, discretisation effects or sparseness (non-extremality of interesting structures). A recognition rate of 72% is claimed, and no information is given if the image data set contains blurred images.

Chen *et al.* [180] devised an approach for text detection treating edge-enhanced Maximally Stable External Regions as basic letter objects. These objects were then filtered using geometric and stroke width information to exclude non-text objects. The performance score that is achieved is 95%.

5.3 Orientation detection and correction

We start by reproducing the concept of Radon Transform, in this context, followed by orientation detection and correction method. Our method use Radon Transform to detect the orientation angle of the skewed text, written on number plate.

5.3.1 Radon Transform

Global detection problem in the image domain is a challenging task. Radon Transform solves this problem by converting it into a more easily solvable local peak detection problem in the parameter domain. After thresholding the Radon transform, the image parameters can be recuperated.

Several existing algorithms can be used to estimate the image parameters like edge detection filters [181], followed by techniques, to connect the individual pixels together, and using linear regression. Such algorithms fail with intersecting lines, when noise level is high and it is difficult to stabilize the edge detection filters. Radon Transform is capable to overcome such problems. If A and B are two finite sets with cardinality $|A|$ and $|B|$, then there are $|B|^{|A|}$ distinct maps from A into B .

A line l in \mathbb{R}^2 can be parameterized by:

$$b = \hat{\xi}(\theta) \cdot \mathbf{x} = x \cos \theta + y \sin \theta$$

where,

$$\mathbf{x} = (x, y)$$

b : distance to the origin along the line perpendicular to l

$\hat{\xi}(\theta) = (\cos \theta, \sin \theta)$: unit vector, indicates the direction of this line

The 2-dimensional Radon Transform is a kernel transformation defined by

$$\mathcal{R} : \mathbb{R}^{\mathbb{R}^2} \rightarrow \mathbb{R}^{\mathbb{R} \times S}$$

$$\mathcal{R}[f](b, \hat{\xi}) = \int_{\mathbb{R}^2} f(x) \delta(b - \hat{\xi} \cdot x) dx$$

f : function defined in some domain of \mathbb{R}^2 .

The Radon transform of the Dirac delta function centered at $\mathbf{x} = \mathbf{x}_0$ is

$$\begin{aligned} \mathcal{R}[\delta(\mathbf{x} - \mathbf{x}_0)](b, \hat{\xi}) &= \int \delta(\mathbf{x} - \mathbf{x}_0) \delta(b - \hat{\xi} \cdot \mathbf{x}) dx \\ &= \delta(b - \mathbf{x}_0 \cdot \hat{\xi}, \hat{\xi}) \end{aligned}$$

The Radon transform of the line indicator function of line $\mathbf{l} = (b_l, \theta_l)$ is

$$\mathcal{R}\{L[\mathbf{l}]\}(b, \hat{\xi}) = \delta(b - b_l, \theta - \theta_l)$$

The Radon transform of the line segment indicator function of segment $\mathbf{g} = (b_l, \theta_l, \chi)$ is

$$\mathcal{R}\{\mathcal{G}[\mathbf{g}]\}(b, \hat{\xi}) = 1_{\{b=b_l, \theta=\theta_l\}}(b, \hat{\xi}) L(\mathbf{g})$$

where,

$$L(\mathbf{g}) = \sum_{\chi \cap S(\mathbf{g})} d\mathbf{x}$$

is the length of segment \mathbf{g} .

The Radon transform of the strip indicator function of strip $\mathbf{s} = (b_s, \theta_s, w_s)$

$$\mathcal{R}\{\mathcal{B}[\mathbf{s}]\}(b, \hat{\xi}) = \begin{cases} \infty & \text{if } |b - b_s| \leq \frac{w_s}{2}, \theta = \theta_s \\ 0 & \text{if } |b - b_s| > \frac{w_s}{2}, \theta = \theta_s \\ \frac{w_s}{|\sin(\theta - \theta_s)|} & \text{if } \theta \neq \theta_s \end{cases} \quad (5.1)$$

The Radon transform of the pixel indicator function of pixel $\mathbf{p}_0 = (0, 0, w, h)$

is

$$\mathcal{R}\{\mathcal{P}[\mathbf{s}]\}(b, \hat{\boldsymbol{\xi}}) = \begin{cases} \frac{h}{|\cos\theta|} & \text{if } 0 \leq |b| \leq \frac{1}{2}(w|\cos\theta| - h\sin\theta) \\ \frac{\frac{1}{2}(w|\cos\theta| + h\sin\theta) - |b|}{|\cos\theta|\sin\theta} & \text{if } \frac{1}{2}|w|\cos\theta| - h\sin\theta| < |b| \leq \frac{1}{2}(w|\cos\theta| + h\sin\theta) \\ \frac{w}{\sin\theta} & \text{if } 0 \leq |b| \leq \frac{1}{2}(h\sin\theta - w|h\cos\theta|) \end{cases} \quad (5.2)$$

The Radon transform of the pixel indicator function of pixel $\mathbf{p} = (p_x, p_y, w, h)$ is

$$\mathcal{R}\{\mathcal{P}[\mathbf{s}]\}(b, \hat{\boldsymbol{\xi}}) = \begin{cases} \frac{h}{|\hat{\boldsymbol{\xi}} \cdot \mathbf{e}_x} & \text{if } 0 \leq d \leq \frac{1}{2}|\hat{\boldsymbol{\xi}} \cdot \mathbf{v} \\ \frac{\frac{1}{2}|\hat{\boldsymbol{\xi}} \cdot \mathbf{u} - d}{(|\hat{\boldsymbol{\xi}} \cdot \mathbf{e}_x)(|\hat{\boldsymbol{\xi}} \cdot \mathbf{e}_y)} & \text{if } \frac{1}{2}|\hat{\boldsymbol{\xi}} \cdot \mathbf{v} < d \leq \frac{1}{2}|\hat{\boldsymbol{\xi}} \cdot \mathbf{u} \\ \frac{w}{\frac{1}{2}|\hat{\boldsymbol{\xi}} \cdot \mathbf{e}_y} & \text{if } 0 \leq d \leq -\frac{1}{2}|\hat{\boldsymbol{\xi}} \cdot \mathbf{v} \end{cases} \quad (5.3)$$

where $\mathbf{c}_p = (p_x, p_y)^T$, $\mathbf{e}_x = (1, 0)^T$, $\mathbf{e}_y = (0, 1)^T$, $\mathbf{u} = (w, h)^T$, $\mathbf{v} = (w, -h)^T$, $|\hat{\boldsymbol{\xi}}| = (|\cos\theta|, \sin\theta)^T$, $d = |b - \hat{\boldsymbol{\xi}} \cdot \mathbf{c}_p|$

5.3.2 The proposed method

The steps involved in orientation detection and correction are shown in figure 5.1.

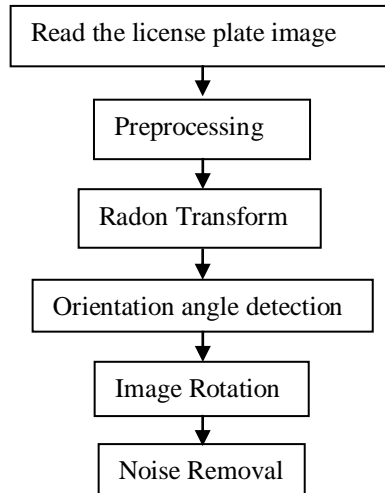


Figure 5.1: Block diagram of orientation detection & correction

5.3.2.1 Read the license plate image

The license plate image I , which needs to be recognized, is read. There are several methods available to localize the license plate from a car image, we use the method given in [87]. If the image is 3-dimensional, we convert it into 2-dimensional. The 2-dimensional tilted license plate is extracted from the car image and is shown in figure 5.2.

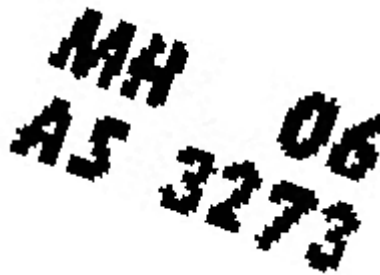


Figure 5.2: License plate image, I

5.3.2.2 Pre-processing

The extracted license plate is put under threshold in this phase for binarization. After binarization, we divide the license plate in two halves I_1 and I_2 and compute the sum of pixel intensities of each row, for each image. The images I_1 and I_2 are shown in figure 5.3. Then the sum of pixel intensities of each row for these two images is compared. Let $S_{I_{1i}}$ and $S_{I_{2i}}$ be the sum of pixel intensities of i th row of I_1 and I_2 image respectively. If we get $S_{I_{1i}} < S_{I_{2i}}$ for the first difference, then the image is oriented in clockwise direction, else in anticlockwise direction. Now invert the pixel intensities of the image I , to get the inverted image as shown in figure 5.4.

5.3.2.3 Radon transform

In this step, we take the Radon transformation of the license plate, the result is shown in figure 5.5.

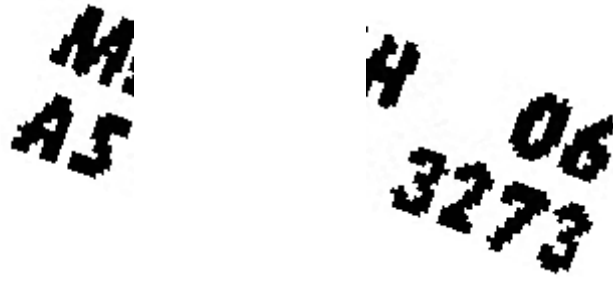


Figure 5.3: (a) First half image of I , I_1 . (b) Second half image of I , I_2



Figure 5.4: Inverted image I' of I

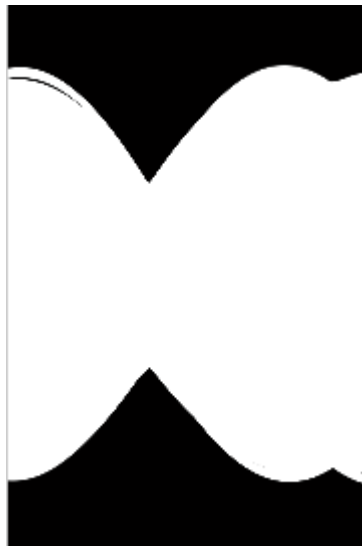


Figure 5.5: Radon Transformation of I'

5.3.2.4 Orientation angle detection

In this step, we find the pixel of maximum intensity in the image created after Radon transformation. Then we find the column in which this maximum intensity

pixel lies. To find the maximum intensity pixel value, search the maximum intensity pixel column-wise and put in the array, thereafter finding the maximum from this array, say A, we search the maximum intensity pixel from the transformed image. The result of plot of the array A is shown in figure 5.6. Now search this number column-wise and stop where it meets to compute the column index. From figure 5.6, it can be seen that the maximum column index is 71 degree.

This column index is the angle, α subtract the angle by 90 degree, which gives the oriented angle, θ .

$$\theta = 90 - \alpha$$

5.3.2.5 Image rotation

Rotate the image in the appropriate direction, as computed in Pre-processing phase, to get the non-skewed image, as shown in figure 5.7.

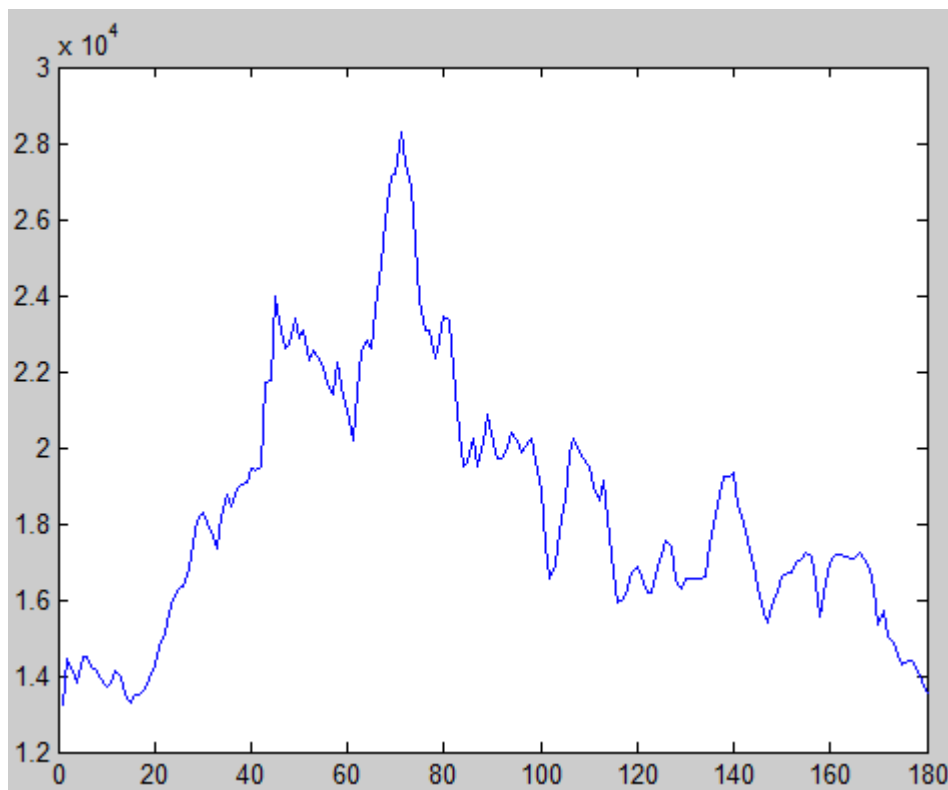


Figure 5.6: Plot of an array A



Figure 5.7: Image after rotation

5.3.2.6 Noise removal

This image becomes blurred due to the noise created by rotating, as shown in figure 5.7. For proper recognition, noise in the image needs to be filtered. The median filter is normally used to reduce noise in an image, somewhat like the mean filter. However, it often does a better job than the mean filter of preserving useful detail in the image.

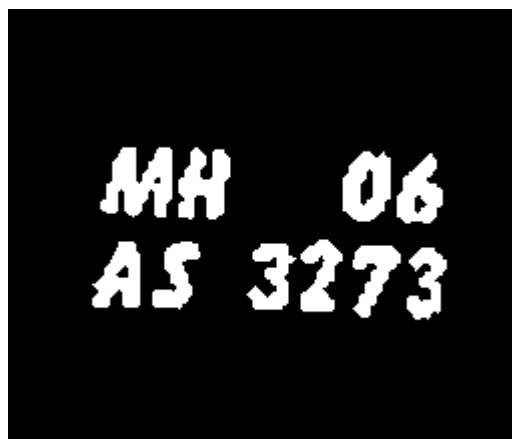


Figure 5.8: Image after noise removal

The median filter works like the mean filter. It looks the nearby neighbours of

each pixel of the image to verify whether it is a representative of its surroundings. It replaces the pixel intensity with the median of neighbouring pixel intensities, instead of the mean value. To compute the median, the pixel values of the nearest neighbour are sorted and then the considered pixel is replaced with the middle pixel value. If there are even numbers of pixels around the candidate pixel, the average of the two middle pixel values is used. We use the median filter to remove the noise from the rotated image. The result is shown in figure 5.8.

5.4 Experimental Results

We applied the proposed technique on 350 tilted number plates, having different orientation angle and direction to measure its accuracy. The input images are colored and black and white images with the size 156×218 pixels. The results are summarized in table 5.1.

5.5 Conclusion

A new technique for the orientation of the license plate detection and then the corresponding correction is proposed in this chapter. For simplicity the task has been divided into six steps: read the license plate image; preprocessing; Radon transform; orientation angle detection; image rotation; noise removal. The existing approaches for license plate recognition do not focus on the tilted license plates and hence they fail to recognize the text of the tilted plate. Hence recognizing the tilted license plates is another challenging task faced by the computer vision now a days. We have used Radon transform to deal with. The technique shown, is tested on 350 tilted images under varying orientation and color, and hence is useful for real life problems.

The results achieved by our technique are venerable. The achieved accuracy of orientation detection is 98.00%; orientation correction is 98.00% and noise filtering is 96.57% as shown in table 5.1.

Table 5.1: Results of Plate orientation detection, correction and noise filtering

	Quantity	Percentage
Total number of available plate images	350	100
Correctly found orientation of plate images	343	98.00
Plate images whose correct orientation were not found	7	2.00

(a) Results of Plate orientation detection.

	Quantity	Percentage
Total number of available plate images	350	100
Correctly found orientation of plate images	343	98.00
Plate images whose correct orientation were not found	7	2.00

(b) Results of Plate orientation correction.

	Quantity	Percentage
Total number of available plate images	350	100
License plates, whose noise filtering has been done successfully for its recognition	338	96.57
License plates, whose noise filtering has not been done successfully for its recognition	12	3.43

(c) Results of Plate noise filtering.